Liposomal trichostatin A: therapeutic potential in hormone-dependent and -independent breast cancer xenograft models

Giorgia Urbinati, Véronique Marsaud, Valérie Nicolas, Juliette Vergnaud-Gauduchon, Jack-Michel Renoir

Horm Mol Biol Clin Invest 2011;6(2):215–225 © 2011 by Walter de Gruyter • Berlin • New York. DOI 10.1515/HMBCI.2011.005

Liposomal trichostatin A: therapeutic potential in hormone-dependent and -independent breast cancer xenograft models

Giorgia Urbinati[1,2], Véronique Marsaud[1,3], Valérie Nicolas[3], Juliette Vergnaud-Gauduchon[1–3] and Jack-Michel Renoir[1,3,*]

[1]Centre National de la Recherche Scientifique, UMR8612 Châtenay-Malabry, France
[2]Paris-Sud University, Orsay, France
[3]IFR 141, Châtenay-Malabry, France

Abstract

Background: Trichostatin A (TSA) is one of the most potent histone deacetylase inhibitors (HDACi) in vitro but it lacks biological activity in vivo when injected intravenously owing to its fast metabolism.

Materials and methods: TSA was incorporated into Stealth® liposomes (TSA-lipo) at a high loading and its anticancer activity was evaluated in several types of breast cancer cells and xenografts.

Results: In estrogen receptor α (ERα)-positive MCF-7 and T47-D cells, TSA induced a long-term degradation of cyclin A and a proteasome-dependent loss of ERα and cyclin D1, allowed derepression of $p21^{WAF1/CIP1}$, HDAC1 and RhoB GTPase, concomitantly with blockade in G2/M of the cell cycle and apoptosis induction. In MDA-MB-231 (MDA) and SKBr-3 cells, TSA increased ERα mRNA and $p21^{WAF1/CIP1}$ protein expression, but decreased cyclin A with a G2/M blockade and cleavage of polyADP-ribose polymerase (PARP). No significant restoration of any ER protein was noticed in any cells. TSA-lipo markedly inhibited tumor growth in MCF-7 and MDA cells xenografts following intravenous injection. Their anticancer effects were characterized by inhibition of Ki-67 labeling, the inhibition of tumor vasculature and an increase of $p21^{WAF1/CIP1}$ in both tumors. In MCF-7 cell tumors, enhanced RhoB accumulation in the cytoplasm of epithelial cells was noticed, inversely to ERα that was strongly decreased.

Conclusion: Such anticancer activity of TSA-lipo is explained by the protection provided by HDACi encapsulation and by the strong tumor accumulation of the nanocarriers as revealed by fluorescence confocal microscopy experiments. Together with its lack of toxicity, the enhanced stability of TSA-lipo in vivo justifies its development for therapeutic use in the treatment estradiol-dependent and -independent breast cancers.

*Corresponding author: Jack-Michel Renoir, INSERM U479, 59 rue Camille Desmoulins, 94805 Villejuif Cedex, France
Phone: +33 (0) 1 4211 4141, Fax: +33 (0) 1 4211 5308,
E-mail: jack-michel.renoir@igr.fr
Received October 11, 2010; accepted January 12, 2011; previously published online March 8, 2011

Keywords: breast cancer; liposomes; trichostatin A; xenografts.

Abbreviations

HDAC	histone deacetylase
HDACi	HDAC inhibitor
TSA	trichostatin A
ER	estrogen receptor
Rhod-PE	L-α-phosphatidylethanolamine-*N*-(lissamine rhodamine B-sulfonyl) (ammonium salt)
$DSPE\text{-}PEG_{2000}$	1,2-distearoyl-*sn*-glycero-3-phosphoethanolamine-*N*-[methoxy(polyethylene glycol)-2000] (ammonium salt)
ePC	egg phosphatidylcholine
Chol	cholesterol
DAB	diamine-3,3-benzidine tetrachlorhydrate
Hsp90	heat shock protein of 90 kDa

Introduction

Approximately 70% of breast cancers (BC) express estrogen receptors (ER), α and β subtypes, that belong to the nuclear superfamily of ligand-induced transcription factors. Since activation of ERα leads to cell proliferation, ERα has long been considered as a risk factor for the development of BC, a risk that is thought to depend upon the ERα/ERβ protein ratio [1]. ERα and ERβ differentially regulate BC cell proliferation as well as apoptosis [2], and ERβ is suspected to act as a tumor suppressor [3–5]. The remaining 30% of BCs are characterized by the absence of ER and by their 17β-estradiol (E_2)-independent growth, leading to a more aggressive phenotype [6, 7]. Endocrine therapy has proven efficient in BCs expressing ERα. However, despite ER expression, antihormone resistance always occurs over time and undesirable side effects have prompted pharmaceutical research to develop new therapeutic strategies. Among them, the combination of various drugs targeting different pathways has appeared attractive, such as the case of hormone therapy combined with molecules that block growth factor receptor signalling and downstream mammalian target of rapamycin (mTOR) [8]. Antibodies (trastuzumab, bevacizumab, IMC-A12, etc.) against these tyrosine kinase membrane receptors [epidermal growth factor receptor (EGFR), vascular endothelia growth factor receptor (VEGFR), insulin-like growth factor receptor (IGFR)] as well as chemical tyrosine kinase inhibitors (gefitinib, sunutinib, etc.) are actually the subject of extensive pre-clinical trials in association or not with anti-estrogen (AE), aromatase inhibitor (AI) or chemotherapeutic

molecules such as taxanes, metabolic inhibitors or anthracyclines. Other drugs inhibiting kinases such as Src and key proteins regulating multiple pathways involved in cell survival such as the proteasome, 90 kDa heat shock protein (Hsp90), farnesyltransferases and histone deacetylase (see http://www.clinicaltrials.gov) are also in clinical trials. In this respect, histone deacetylases (HDAC) have been considered as an important target for the development of anticancer drugs because deacetylation of histones is responsible for silencing a number of genes that inhibit cellular growth as a result of a closed chromatin configuration, which is unfavorable for transcription [9]. Thus, HDAC inhibitors (HDACi) reverse this process and inhibit tumor growth by causing repression of certain oncogenes such as c-myc [10] but activation of others such as the cyclin-dependent kinase inhibitor $p21^{WAF1/CIP1}$ [11]. Moreover, HDACi have been shown to affect the cell cycle, programmed cell death [12–14], differentiation and angiogenesis in many cancer cells as well as in vivo [14, 15].

HDACs are classified into four classes containing different enzymes with various cell localization: class I (HDAC1, 2, 3 and 8); class IIa (HDAC4, 5, 7 and 9); class IIb (HDAC6 and 10); and class IV (HDAC11). HDACs oppose dynamically their activity to that of histone acetyl transferases (HAT) by inducing a condensed chromatin structure which impairs access of transcription factors to DNA; on the contrary, HATs enhance acetylation of histones, leading to an open chromatin conformation allowing binding of transcription factors to DNA [16]. Furthermore, the fate and therefore the activity of non-histone proteins such as the transcription factors p53 [17], androgen receptor [18] and ERα [19–23] is known to be regulated through HDAC-mediated hypoacetylation. Indeed, several laboratories have shown that acetylation modulates the ERα transactivating capacity in BC cells. In addition, HDACi cause hyperacetylation of Hsp90, Raf, Akt, ErbB2 and Bcr-Abl, enhancing their antitumor effects [24].

HDACi are classified into six classes based on their chemical structures; the largest class is that of hydroxamates to which trichostatin A (TSA) belongs [15]. TSA is an inhibitor of numerous zinc-dependent, class I and II HDACs. Unfortunately, TSA has been shown to be devoid of any biological activity in mice xenografted with cancer cells when injected intravenously [25–27] owing to its fast metabolism in vivo [28, 29], and clinical trials with this inhibitor have been abandoned.

We recently incorporated TSA at a high-dosage into pegylated liposomal formulations [30]. These TSA-loaded "Stealth®" liposomes (TSA-lipo) are highly stable in vitro and release TSA slowly. Data support a prolonged antitumor activity of pegylated TSA liposomes and confirm that this type of formulation protects the drug from inactivation. Immunohistochemistry allowed detection of re-expression of the CDK inhibitor $p21^{WAF1/CIP1}$ in both MCF-7 and MDA cells tumors, whilst the small GTPase RhoB was strongly enhanced in MCF-7 tumors concomitantly with destruction of ERα protein, suggesting an inverse relationship between ERα and the putative tumor suppressor RhoB. Altogether, these results support the usefulness of evaluating TSA-loaded liposomes in clinical trials both in estrogen-dependent and -independent human BCs.

Material and methods

Chemicals

TSA was obtained from Alomone Labs (Jerusalem, Israel). Rhod-PE, ePC and DSPE-PEG_{2000} were purchased from Avanti Polar Lipids (Alabaster, AL). DAB and Chol were obtained from Sigma-Aldrich (St Quentin-Fallavier, France). All other chemicals were reagent grade purchased from standard suppliers.

Liposome fabrication

Liposome suspensions (50 mM lipids) were prepared by lipid film hydration at the following molar ratios: ePC/Chol/DSPE-PEG_{2000} (64:30:6, w/w) as described previously [31] and modified according to procedures of Urbinati et al. [30]. For Rhod-PE-labeled liposomes, Rhod-PE lipid (0.5% of the total molar lipid ratio) was added into the chloroformic lipid solution instead of TSA.

Cell culture treatments

MCF-7, T47-D, SKBr-3 and MDA-MB-231 (MDA) cell lines (ATCC, Molsheim, France) were cultured in Dulbecco's modified Eagle's medium (DMEM) (Lonza Verviers, Verviers, Belgium) supplemented with penicillin (5 IU/mL), streptomycin (50 IU/mL) and 10% fetal calf serum (FCS). Prior to treatment, the medium was replaced with phenol red-free DMEM medium containing 10% stripped FCS (Norit A charcoal 1%, dextran T-70 0.1%, 30 min at room temperature) for at least 48 h.

Immunoblotting

Cells were lysed and the protein concentration was quantified as described by Marsaud et al. [32]. Protein content from total cell extracts (30 μg) was separated by sodium dodecyl sulfate polyacrylamide gel electrophoresis (SDS-PAGE) and was electrotransferred onto a polyvinylidene difluoride membrane (Immobilon® P; Millipore Corp., Saint-Quentin-en-Yvelines, France). The membrane was blocked for 1 h at 37°C in 10% dried non-fat milk in phosphate-buffered saline containing 1% Tween 20 (PBST) or 5% FCS, depending on the first antibody, and further incubated for 45 min at room temperature with anti-ERα (HC-20, 0.1 μg/mL), anti-$p21^{WAF1/CIP1}$ (N-20, 1 μg/mL), anti-cyclin D1 (HD11, 1 μg/mL), anti-cyclin A (BF683, 0.5 μg/mL), anti-RhoB (C5, 1 μg/mL), anti-polyADP ribose polymerase (PARP) (F2, 0.5 μg/mL) or anti-Hsp70 (W27, 1 μg/mL) (all purchased from Santa Cruz Biotechnology, Santa Cruz, CA, USA), or anti-acetyl-histone H4 (07-328, 0.1 μg/mL) or anti-HDAC1 (07-643, 0.1 μg/mL) (both from Upstate, Temecula, CA, USA), or anti-ERβ [either a rabbit polyclonal antibody at 1/5000 dilution (gift from P. Chinestra and J-C Faye, Claudius Regaud Institute, Toulouse, France) or rabbit polyclonal Ab3577 (Abcam-PLC, Paris, France) at 1 μg/mL]. Appropriate horseradish peroxidase-conjugated secondary antibodies (45 min incubation at room temperature) and Luminol reagent (Santa Cruz Biotechnology) were used for detection.

Flow cytometry experiments

Cells ($1-1.5\times10^5$ cells/mL) were cultured in the absence (control) or presence of free HDACi, encapsulated HDACi or empty liposomes at the same lipid concentration. After treatment, cells were washed and fixed in PBS/ethanol (30%/70%). Cells (10^4) were then incubated for 30 min in PBST/Triton X-100, 0.2% ethylene diamine tetra-acetic acid (EDTA) and 1 mM propidium iodide (50 μg/mL) supplemented with RNase (0.5 mg/mL). Analyses were performed with a BD FACSCalibur™ flow cytometer (Becton Dickinson, Le Pont-de-Claix, France). CellQuest software was used for data acquisition and analysis.

Reverse transcriptase polymerase chain reaction (RT-PCR) and quantitative PCR (qPCR)

Total RNA was extracted from 10^6 cells with TRIzol® reagent according to the manufacturer's instructions (Invitrogen, Carlsbad, CA, USA). One microgram of total RNA was subjected to reverse transcription using random primers (Invitrogen). Primers for amplification of target genes were as follows: ERα, forward AGACATGAGAGCTGCCAACC and reverse GCCAGGCACATTCTAGAAGG (1214–1512); ERβ, forward TCACATCTGTATGCGGAACC and reverse CGTAACACTTCCGAAGTCGG (704–1049); and β-actin, forward TGACGGGGTCACCCACACTGTGCCCATCTA and reverse CTAGAAGCATTTGCGGTGGACGATGGAGGG (542–1202). PCR was performed for 30 cycles with 1 min in denaturing conditions at 94°C, annealing at 65°C and extension at 72°C, and results were analyzed by 2% agarose gel electrophoresis. For quantitative real-time PCR, experiments were carried out with a LightCycler® system (Roche Diagnostics, Meylan, France) using the LightCycler® FastStart DNA Master SYBR Green I Kit (Roche Diagnostics, Meylan, France) according to the manufacturer's instructions. In addition to the ER primers described above, 36B4 primers were also used as controls (forward GATGCCCAGGGAAGACAG and reverse TCTGCTCCCACAATGAAACAT). Cycles were as follows: a 10 min initial cycle at 95°C, followed by 45 cycles of 10 s denaturation at 95°C, 5 s annealing at 58°C and 10 s extension at 72°C. The specificity of the fluorescence was verified by melting curve analysis after each reaction. The relative abundance of each target was normalized to 36B4 expression and the quantity of each mRNA compared with 36B4 was done using the comparative threshold method (Ct).

Xenografts and treatments

MCF-7 ($5-10\times10^6$/mL) or MDA ($1-2\times10^7$/mL) cells were mixed with an equal volume of Matrigel™ (BD Biosciences, Le Pont-de-Claix, France) and were injected (200 μL total) subcutaneously in the vicinity of the nipples of 6-week-old female nude mice (Janvier, Le Genest Saint-Isle, France). MCF-7 xenografts were treated weekly with 20 μL of a 10^{-2} M ethanolic solution of E_2 applied to the neck skin. Once tumor volumes reached 300–500 mm^3 [calculated as 1/2 (width × length^2)], mice (6 per group) were treated with TSA-lipo (containing 0.01 mM or 1 mM TSA) or empty liposomes administered twice a week intravenously (100 μL) into the retro-orbital sinus.

Tumor progression was determined by the ratio of tumor volume at each time point to initial tumor volume at week 0 (start of treatment). At the end of the experiment, tumors were excised and portions were fixed either in FineFIX (Milestone s.r.l., Sorisole, Italy) or in paraformaldehyde. Experiments were carried out in compliance with the recommendations of the European Economic Community (86/609/EEC) and the French National Committee (decree 86/848) for the care and use of laboratory animals.

In vivo liposome uptake

Rhod-PE-labeled liposomes were injected intravenously into mice bearing MCF-7 cells tumors and were then excised at 1 h or 24 h and treated as described previously [33]. Tumor slices were observed with an inverted LSM-510 META confocal laser scanning microscope (Zeiss, Stuttgart, Germany) equipped with a helium-neon laser (excitation wavelength 543 nm) using a Plan-Apochromat 63× objective lens (NA 1.40, oil immersion). Rhodamine fluorescence was collected with a 560 nm Long Pass emission filter. The pinhole diameter was set at 106 μm. Stacks of images were collected every 0.41 μm along the z-axis, and 12-bit numerical images were acquired with LSM 510 software version 3.2.

Immunohistochemistry of tumor sections

FineFIX-fixed, paraffin-embedded tumors were cut in 4-μm thick sections and detection of Ki-67 (anti-Ki67, 1:75; DAKO, Glostrup, Denmark), CD34 (anti-mouse CD34, 1:20; HyCult Biotech b.v., Uden, The Netherlands), $p21^{WAF1/CIP1}$ (anti-$p21^{WAF1/CIP1}$, 1:50; Cell Signalling, Danvers, MA), ERα (anti-ERα H-184, 1:100; Santa Cruz Biotechnology) and RhoB (anti-RhoB C5, 1:20; Santa Cruz Biotechnology) was carried out as described previously [34]. Staining was revealed using the Vectastain® Kit (Vector Laboratories, Burlingame, CA) using DAB as a chromogen. Slides were counterstained with Mayer's hemalum and mounted (Eukitt®; O. Kindler GmbH, Freiburg, Germany). All slides were examined using a Nikon eclipse TE2000-S microscope. For each specimen, five contiguous fields were digitised and analyzed.

Quantification and statistical analyses

Quantification of Western Blot signals was performed using Bio-Profil V99 1D software from Wilbert Lourmat (Fisher BioScientific, Illkirsh, France). Statistical significance was estimated by the two-tailed t-test using Microsoft Excel (Microsoft Corp., Redmond, WA, USA). Differences were considered significant at $p<0.05$ and $p<0.01$.

Results

In vitro activity of TSA in breast cancer cells

PCR In preliminary experiments, the ER status of each cell line (MCF-7, T47-D, SKBr-3 and MDA) was established both by PCR and Western blot. As shown in Figure 1A, both ER isotypes were detected in MCF-7 cells. TSA, whether free or encapsulated, did not significantly modify the mRNA pattern in MCF-7 and MDA cell lines (Figure 1A). Data similar to those obtained with MCF-7 cells were obtained with T47-D cells (not shown). However, despite several attempts, it was difficult to obtain a quantitative estimation of ER mRNA levels after stimulation of both cell lines with 0.5 μM TSA, whether free or encapsulated. In contrast, in MDA cells, as well as in SKBr-3 cells (not shown), only ERβ mRNA was detected. No clear difference in mRNA levels of each type of ER was observed in cells exposed both to free TSA and liposome-entrapped TSA.

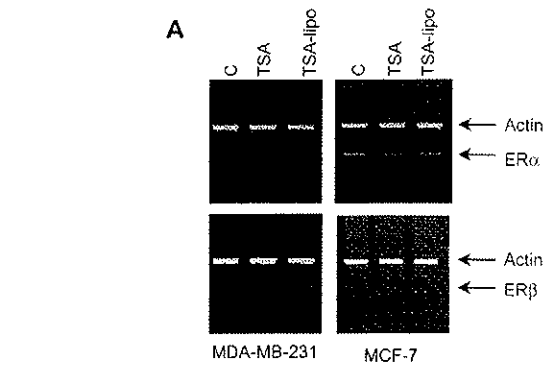

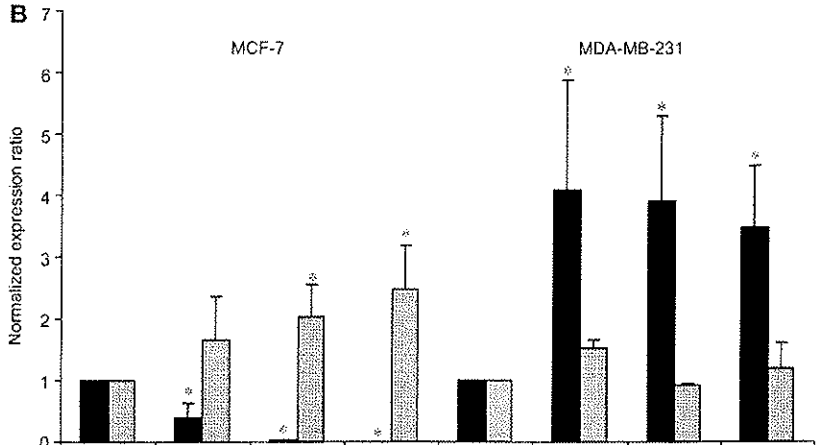

■ ERα	1	0.39±0.23	0.017±0.01	0.09±0.0	1	4.09±1.77	3.89±1.414	3.47±1.0
⊡ ERβ	1	1.65±0.71	2.04±0.52	2.48±0.70	1	1.52±0.14	0.92±0.03	1.18±0.42

Figure 1 Effect of trichostatin A (TSA) on estrogen receptor α and β (ERα and ERβ) expression in breast cancer cells.
(A) MCF-7 and MDA-MB-231 (MDA) cells were exposed or not (control, C) to free TSA or encapsulated TSA (TSA-lipo) at 0.5 μM for 24 h. ER mRNA was quantified with reference to the housekeeping β-actin gene as described in the Materials and methods. (B) MCF-7 and MDA cells were exposed or not (vehicle alone) to various concentrations of TSA for 24 h and RNA was prepared and submitted to real-time polymerase chain reaction (PCR) as described in the Material and methods. For each treatment, two different cell cultures were analyzed in duplicate (4 RT) and were normalized to 36B4. Fold change of ΔCt (Ct ER–Ct 36B4) are values in the table corresponding to each bar of the histogram. 36B4 was chosen in quantitative PCR because the intensities of the Ct were higher than those obtained with reference to actin. * and ** indicate statistical significance of the difference between the average of experiments with the average of the controls (vehicle) by t-test (*$p<0.05$; **$p<0.01$). Note that comparable results to those obtained with MCF-7 and MDA cells were obtained with T47-D and SKBr-3 cells, respectively.

qPCR Expecting to achieve better quantification, qPCR was performed on mRNA from cells exposed to various concentrations of free TSA. As shown in Figure 1B, a significant decrease of ERα mRNA occurred in treated MCF-7 cells compared with untreated cells. Moreover, a very small increase of ERβ mRNA was noticed, appearing significant at 2 μM TSA. In contrast, in MDA cells ERα expression was found to be significantly enhanced already at 0.5 μM TSA, but no significant increase of ERβ was observed.

Western blotting ERβ protein was undetectable in MCF-7, MDA, T47-D and SKBr-3 cells whatever the antibody used (not shown), and ERα was immunostained only in MCF-7 (Figure 2) and in T47-D cells (not shown); this indicates a very low expression level of both ERs, if any, in MDA cells, or a fast turnover of ER proteins in this latter cell line. As a positive control, TSA induced a dose-dependent acetylation of histone H4. In parallel, a dose-dependent and MG132-sensitive degradation of ERα [calculated 50% inhibitory concentration (IC_{50}) = 0.35 μM] in MCF-7 and T47-D [30] cells was observed. Such a decrease of ERα protein is in agreement with the decrease of mRNA shown in Figure 1. Moreover, cyclin D1 and cyclin A (in all cells) were also downregulated by TSA, but only cyclin D1 was

targeted to a proteasome-mediated degradation, in agreement with previous data [35]. The cell cycle inhibitor $p21^{WAF1/CIP1}$ is poorly expressed in MCF-7 cells [36] but its expression was strongly and dose-dependently augmented by TSA in both cell lines. This is in agreement with previous reports showing the requirement of $p21^{WAF1/CIP1}$ for butyrate-mediated inhibition of human colon cancer cell proliferation [37], its selective induction by HDACi as well as gene-associated histone acetylation [38] and also with the capacity of suberoylanilide hydroxamic acid (SAHA) to increase its expression in SKBr-3 and BT-474 BC cells [39]. The GTPase RhoB, suspected to act as a tumor suppressor in human cancer cells [40], was re-induced in MCF-7 cells, but not in MDA cells in which it was not immunodetectable (Figure 2A and 2B). Similar results on RhoB enhancement were obtained with increasing doses of other HDACi such as PXD-101 and CG-1521 (not shown).

Differences in the data between mRNA expression (Figure 1) and ER protein (Figure 2) are difficult to explain, even if the significance tests are in favor of a restoration of ERα mRNA in MDA cells. Indeed, data from others showed that ER-negative BC cells exposed to HDACi such as valproic acid or SAHA [39, 41], in association [25, 42] or not [43] with the DNA methyltransferase inhibitor 5-aza-2'-deoxycytidine (5-Aza), led to an increase in both ER proteins. Other published [44] and unpublished (G. Lazennec, personal communication) works studying TSA treatment of a number of BC cells do not agree with these findings. It is evident that both ERβ mRNA and protein levels are low, even after TSA treatment, and the high sensitivity of qPCR may detect low variations that cannot be seen at the protein level. Similarly, expression of ERα in MDA cells may be enhanced upon TSA exposure but to a small extent, and a fast protein turnover may impair its detection by Western blot.

A TSA dose-dependent cleavage of PARP occurred in MDA cells but not in MCF-7 cells (Figure 2). The fact that PARP is cleaved in MDA cells supports a mitochondrial-induced apoptotic process as described previously [42, 45]. In contrast, no PARP cleavage was noticed in MCF-7 cells. Taken together with the results in Figure 3, these data argue for TSA-induced cell death in both cell lines.

We also checked for the activity of TSA upon the stability of HDAC1, since expression of this HDAC was reported as being controlled by RhoB [46] and to be released from the ERα promoter [47]. As shown in Figure 2, HDAC1 is dose-dependently induced by TSA in MCF-7 as well as in MDA cells although to a lesser extent. This effect follows the behaviour of both ERα and RhoB upon TSA exposure of MCF-7 cells, suggesting some interplay between ERα, HDAC1 and RhoB.

Influence of TSA liposomes in cell the cycle of breast cancer cells

We previously showed that TSA as well as two other HDACi (Belinostat® and CG-1521) affect the viability of BC cells. To characterise further the biological activity of TSA-lipo, their effects upon the cell cycle in the same ERα-positive MCF-7 and ERα-negative MDA cells were analyzed. Flow cytometry analysis (Figure 3) indicated that unloaded liposomes had no impact on MCF-7 and MDA cell proliferation as well as on cell death. Importantly, and as expected [36], both free and encapsulated TSA already at 0.5 μM blocked cells in G2/M phase. At a lower concentration (50 nM), TSA caused a weak accumulation of MCF-7 cells in G1 and in G2/M phases while having no effect on MDA cells. In this type of analysis, TSA-lipo led to a higher fraction of cells in sub/G1 in MDA than in MCF-7 cells, and the encapsulation potentiated the activity of TSA, in particular in MCF-7 cells. Moreover, these analyses indicated that, depending on the concentration and on the cell type, TSA does not have the same effect on cell cycle and cell death, confirming the

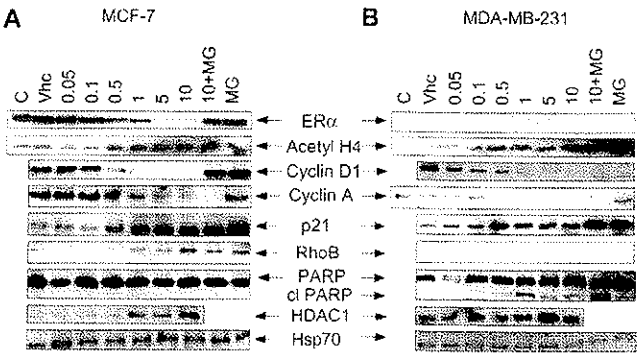

Figure 2 Trichostatin A (TSA) potential on cell cycle protein stability in breast cancer cells.
(A) MCF-7 and (B) MDA-MB-231 (MDA) cells were exposed or not (control, C; or vehicle alone, Vhc) to increasing concentrations of TSA for 20 h in the presence or not of 5 μM of the proteasome inhibitor MG132 (MG). Estrogen receptor α (ERα), cyclin D1, cyclin A, $p21^{WAF1/CIP1}$, polyADP-ribose polymerase (PARP), cleaved PARP (cl PARP), RhoB GTPase, HDAC1 and Hsp70, for control of constant protein loading, were blotted and detected in 30 μg of protein from total cell extracts with relevant horse radish peroxidase-labeled specific antibodies. Detection of acetyl-histone H4 served as a control for the activity of the histone deacetylase inhibitor (HDACi) (augmented 10-fold in MCF-7 cells and 25-fold in MDA cells compared with untreated cells). Blots are representative of at least three independent experiments. $p21^{WAF1/CIP1}$ augmented ×50 in MCF-7 and ×20 in MDA, whilst a 60-fold augmentation of RhoB was estimated in MCF-7 cells. HDAC1 was estimated to augment ×50 and ×10 fold in MCF-7 and MDA, respectively.

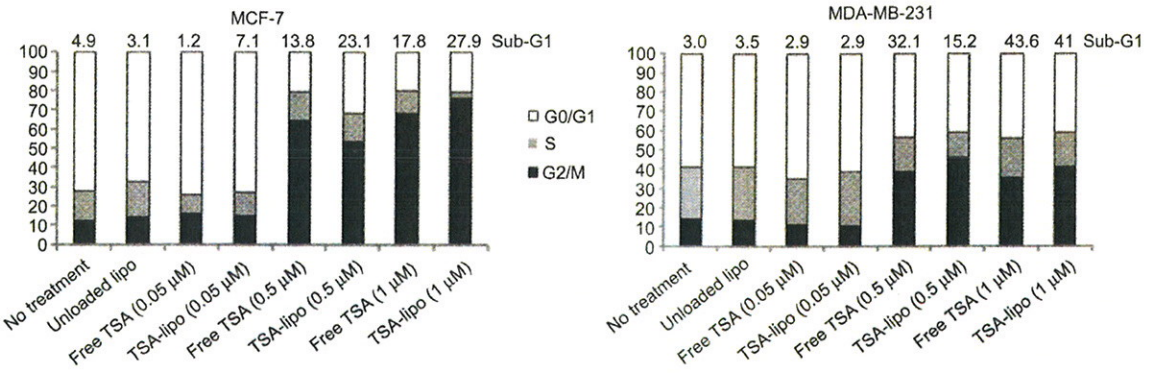

Figure 3 Influence of free and encapsulated trichostatin A (TSA) on the cell cycle and apoptosis.
MCF-7 and MDA-MB-231 cells were plated at a density of 5×10^5 cell/mL and were exposed or not (NT) to free or encapsulated TSA (0.05–1 µM). They were harvested 48 h later, fixed in ethanol and analyzed as described in the Materials and methods. For each series, 10,000–20,000 events were gated. The histograms present the percentage of cells within each phase of the cell cycle and the amount of cells in the sub-G1 fraction. Values are representative of two experiments performed with two independent cell cultures.

results in Figures 1 and 2. Data from Figure 2 suggest that apoptosis in MDA cells could involve the mitochondrial pathway, in agreement with previous data showing that this is due to cleavage (activation) of caspase-3 [42]. The fact that no PARP cleavage was observed in MCF-7 could be due to an insufficient exposure time, since PARP cleavage has been observed in these cells following TSA treatment [42]. However, MCF-7 cells lack caspase-3 [48], and Liang et al. showed that in this cell line the intrinsic apoptotic pathway proceeds through sequential activation of caspase-9 followed by that of caspase-7 and -6 [49]. Whether TSA affects MCF-7 cell death through the intrinsic or the extrinsic pathway remains to be established.

In vivo liposome uptake

We further investigated the behaviour of TSA-lipo in vivo to determine whether they accumulate in tumors. It has been largely documented that after a single intravenous (i.v.) injection of any type of fluorescent-labeled nanoparticle, major capture of the dye is achieved rapidly (first hour) in the liver, followed later by the spleen (see [50] for a review). Unfortunately, we observed a very strong autofluorescence in richly vascularised organs of untreated mice such as the liver, spleen and even the uterus, preventing any further analyses in these organs. We then focused on tumor accumulation of Rhod-PE-labeled liposomes and visualized important clusters of fluorescence around vessels (Figure 4B). Twenty-four hours after injection, Rhod-PE-labeled liposomes were observed in tumors by confocal laser microscopy. Importantly, a decreasing fluorescence gradient was observed around vessels irrigating the tumor as the distance from the capillary increased. This phenomenon was well detectable even 1 h after injection (not shown), although it was less pronounced than at 24 h. This suggests that liposomes accumulate at the tumor site for a long-time after injection, supporting the great stability of Rhod-PE-liposomes and a prolonged time in the blood. Owing to the tumor-specific enhanced permeability retention caused by the discontinuous endothelium facilitating extravasation of liposomes [51], the nanocarriers are believed to cross through the endothelium and to process to endocytosis as shown in vitro here with MCF-7 tumor cells.

In vivo antitumor activity of TSA liposomes in breast cancer xenografts

TSA alone is generally ineffective in inhibiting the growth of solid tumor xenografts [25, 27, 52–54] because of its fast metabolism [28] in vivo; a modest effect was noted with 0.5 mg/kg daily doses of TSA in dimethyl sulphoxide (DMSO) through intraperitoneal injection in rats bearing *N*-

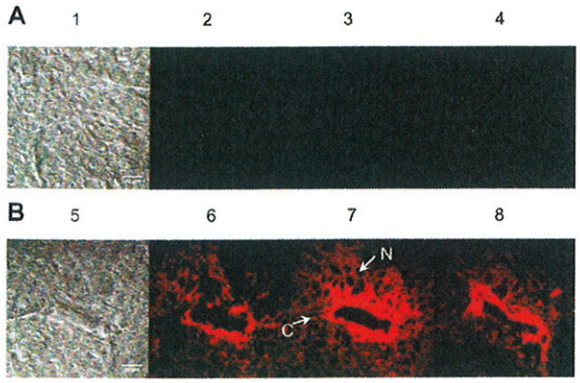

Figure 4 Uptake of fluorescent-labeled liposomes.
Mice bearing MCF-7 cell tumors (n = 3) were i.v. injected (panel B, 5–8) or not (panel A, 1–4) with Rhod-PE-labeled liposomes, and tumors were excised at 24 h. Fluorescence detection by confocal microscopy of tissue at 24 h (63× magnitude) shows a very low auto-fluorescent signal in untreated tumors (panels 2, 3 and 4 in A), whereas a very bright one is observed, for treated tumors, around a blood vessel (panels 6, 7, 8 in B) at different depths of field (2.87, 7.80 and 26.28 µm, respectively). Panels 1 and 5 are differential interferential contrast views of the tissue. Images are representative of three different tumors.

methyl-*N*-nitrosourea carcinogen-induced mammary carcinoma [55, 56]. Therefore, we focused on the activity of intravenously injected liposomal TSA in MCF-7 and MDA xenografts. Free TSA (control) could not be administered intravenously owing to its low solubility in aqueous solutions. As shown in Figure 5, growth of both tumor types was blocked following biweekly treatment with 1 mM TSA-lipo corresponding to a TSA dose of 1.5 mg/kg/week. MCF-7 tumors treated with the lower 10 μM TSA-lipo formulation, corresponding to a TSA dose of 15 μg/kg/week, continued to grow (Figure 5A), suggesting that free liposomes have no intrinsic effects and that a sufficient TSA concentration is needed to achieve antitumor activity. Indeed, after 4 weeks the size of control MCF-7 xenografts increased by 2.5-fold, whilst the volume of TSA-lipo-treated tumors only marginally and non-significantly increased (1.3-fold) (Figure 5A). Similar experiments performed with MDA xenografts, at an equal TSA dose, also showed tumor growth arrest (Figure 5B) even stronger than that obtained with mice bearing MCF-7 cells tumors. All together, these data suggest: first, that the liposome formulation protects the TSA molecule from inactivation in vivo; and second, that TSA liposomes are strong growth inhibitors both of ER-positive and -negative BC cells.

Immunohistochemistry analysis

Figure 6 shows the decrease of the Ki-67 proliferation marker both in MCF-7 and MDA xenografts treated with TSA liposomes, confirming the antiproliferative activity of encapsulated TSA. Unloaded liposomes had no effect on tumor growth and also no effect upon all of the parameters further analyzed. Concomitantly to the decrease of Ki-67 (mean ± standard deviation 60% ± 15% for MCF-7 cell tumors and 78% ± 16% for the MDA tumors; n = 5), a practically complete disappearance of the tumor vasculature was observed, as revealed by the lack of CD34 labeling (< 3% of labeling was counted in five contiguous tumor fields for each type of xenograft). This is in agreement with data showing that HDACi act indirectly upon solid tumor growth by inhibiting neoangiogenesis [57]. This antitumor effect is thought to enhance the activity of entrapped TSA, together with an increase of the CDK inhibitor $p21^{WAF1/CIP1}$ (fold induction × 250 ± 45 in MCF-7 and × 100 ± 22 in MDA tumors compared with untreated tumor labeling) in both the cytoplasm and nuclei of tumor cells independently on the presence of ERs. However, in the case of ER-positive MCF-7 cells tumors, a 85% ± 12% decrease of ERα level and a strong increase of RhoB GTPase (× 50 ± 19; n = 3) expression were observed. RhoB was found mainly localizing in the cytoplasm and at the membrane periphery of tumor cells, in agreement with the already described localization of RhoB [40, 58–60].

Discussion

The present work evaluated the antitumor activity of TSA-loaded liposomes in two types of BC xenografts, which were designed for i.v. administration. These biodegradable pegylated nanocarriers are characterized by their small size (~ 150 nm) and proved to be non-toxic in vitro [30]. TSA was incorporated at a high concentration and remains stable in liposomes for at least 4 weeks [30]. Such a feature is required for efficient biological activity of the nanosystem since the IC_{50} of TSA in terms of HDAC inhibition is close to 0.5 μM [15], implying that relatively high doses are needed to produce a therapeutic effect. Indeed, the potential of these TSA liposomes as an efficient nanocarrier was shown here following i.v. injection of small doses of liposomes as revealed by the arrest of solid BC tumor growth both of estrogen-dependent (MCF-7 cells) and estrogen-independent (MDA cells) xenografts.

Intravenous injection resulted in tumor accumulation via a prolonged blood residency time owing to their ability to resist macrophage capture as already described for the same pegylated liposomes and for pegylated nanoparticles loaded with small hydrophobic molecules [61]. Indeed, liposomes of such a small size are known to extravasate from capillaries, which are often discontinuous in tumors [62]. Once in tumors, TSA liposomes can proceed to endocytosis, releasing the entrapped active molecule inside the cell compartment of

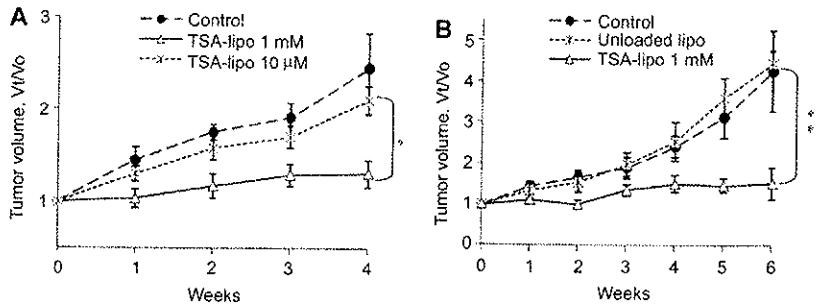

Figure 5 Tumor growth evolution.
Both MCF-7 and MDA-MB-231 (MDA) xenografts (n = 6) were injected intravenously (twice a week) or not with trichostatin A liposomes at different charges of TSA (A,B) or with empty liposomes (B). Tumor volume (mean ± standard deviation) was measured weakly and was plotted against time (weeks of treatment). Evolution curves of MCF-7 and MDA tumors from treated mice were significantly different from those of the control untreated mice at $^{*}p < 0.05$ (A) and $^{**}p < 0.01$ (B).

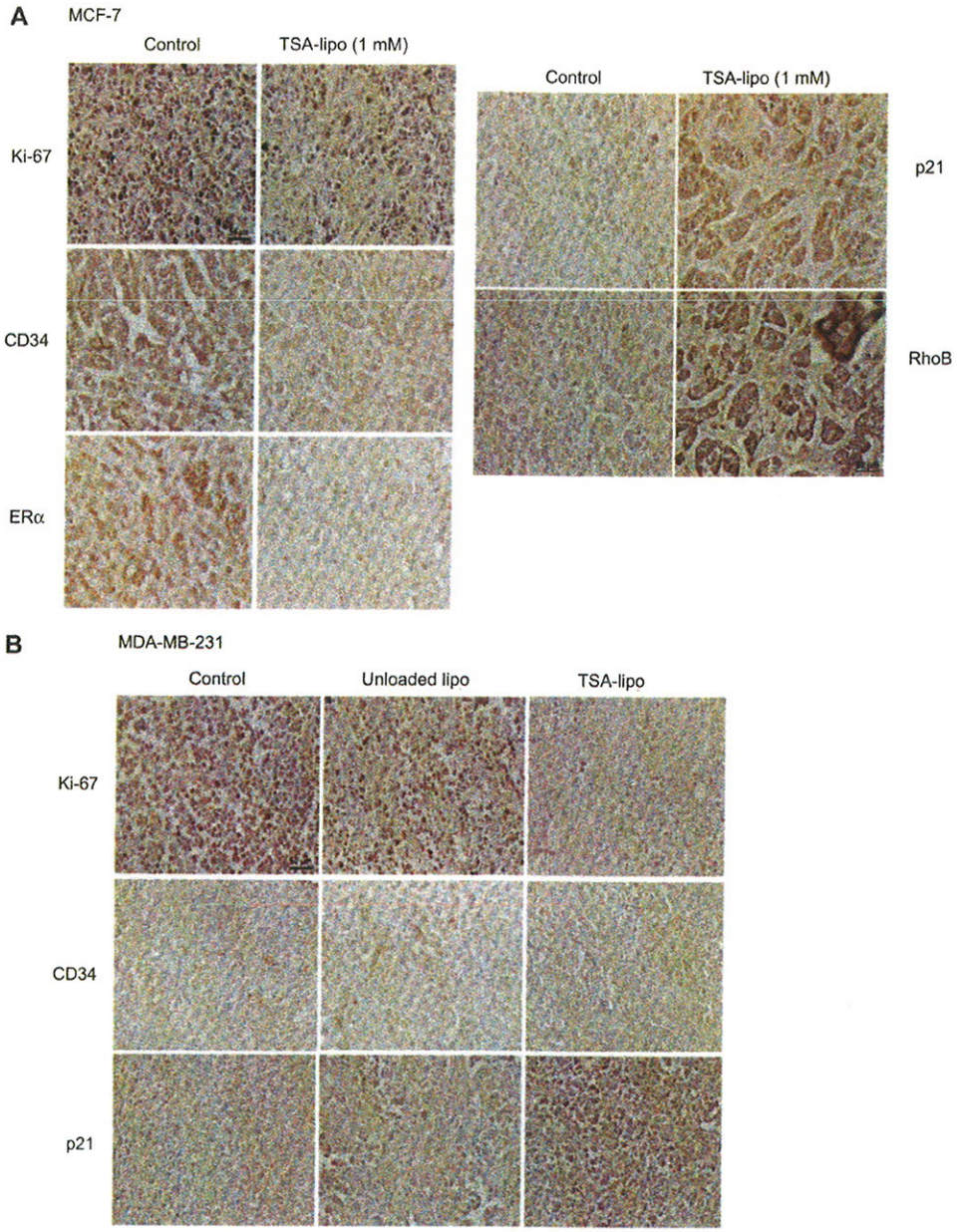

Figure 6 Immunohistochemistry of breast cancer tumors from xenografts treated with trichostatin A liposomes.
(A) MCF-7 cell tumors and (B) MDA-MB-231 cell tumors were analyzed for Ki-67, estrogen receptor α (ERα), $p21^{WAF1/CIP1}$, RhoB and CD34 in the conditions described in the Materials and methods and were compared with immunostaining obtained on untreated tumors (control) or tumors treated with empty liposomes. Magnification was ×200. Vessels are shown in brown in CD34 staining. An insert (×10) in panel (A) for RhoB staining is shown for better visualization of the cytoplasmic localization. The selected pictures were representative of at least five images from five sections per tumor, each taken from three distinct animals belonging to the same group.

tumor epithelial cells. In case of destruction of some liposomes outside the tumor cell, the released drug can then diffuse through the cell membrane owing to its lipophilic property and thereafter reach the molecular target(s) in epithelial, stromal and endothelial cells.

At the molecular level, the decrease of ERα in MCF-7 tumor cells treated by TSA-lipo, together with the increase of $p21^{WAF1/CIP1}$, are in agreement with the suppression of E_2-induced tumor growth, as suggested by experiments performed with BC [63] and colon cancer [37] cells. Moreover, the ER is not the only target of TSA in BC cells. Noteworthy, the antivascular activity of TSA liposomes, revealed by the tumor vessel normalization, constitutes an added value to the TSA-loaded anticancer activity of the nanosystem. This effect could be extended to a number of other solid tumors as sustained here by the results obtained with MDA tumors.

In addition, it is tempting to speculate that TSA-lipo could enhance the activity of tamoxifen since it was shown that TSA could be efficient in the re-expression of ERα [43] or ERβ [22], although it has not been observed in patients. Moreover, we did not detect ERβ protein after TSA treatment either in MCF-7 cells or in tumors. Therefore, the molecular mechanism(s) by which TSA affects BC tumor growth may depend on the BC cell type and probably the expression level of various unidentified factors regulating cell proliferation.

Among them, the small GTPase RhoB protein could play an important role. Loss of RhoB expression frequently occurs in many cancers, whereas its re-expression could be highly significant in suppressing tumor growth as shown in ovarian cancer-bearing mice [64] and in lung NIH3T3 cells [65]. Re-expression of RhoB has appeared of great therapeutic interest. RhoB, like other Rho family proteins, cycles between GTP- (active) and GDP- (inactive) bound states and is controlled by various post-transductional mechanisms, mainly farnesylation and geranylgeranylation through specific enzymes [66]. RhoB interacts with numerous regulators and effectors that modulate activity and influence important processes in cancer, including neoplastic transformation, invasion, survival and metastasis [67, 68]. Contrary to other small GTPases, RhoB is an immediate early response gene in response to various stimuli, including the growth factors epidermal growth factor (EGF) and transforming growth factor β (TGFβ) [69, 70] with a short half-life [71]. Antiestrogens are also known to modulate TGF-β, whose function in BC is still poorly understood since it acts as a potent inhibitor of tumor progression by inducing growth arrest and apoptosis in transformed mammary gland cells [72, 73] and may function as a tumor promoter [74]. However, some reports indicated that overexpression of RhoB is of poor clinical outcome in BC [75] and it has been documented that RhoB could correlate with disease progression [76]. Thus, it is disturbing to observe a regression of ER-positive tumors with simultaneously upregulation of RhoB and downregulation of ERα.

To understand the molecular mechanism(s) by which TSA induces suppression of E_2-induced tumor growth, it could be helpful to look at the expression of direct TSA targets, i.e. HDAC. Several HDACs are directly or indirectly associated with ERα in BC cells and a strong correlation between ER- and progesterone receptor-positive cells with HDAC1 [77] has been evidenced. Thus, it could be important to decipher the relationship between ERs and HDAC1 following TSA, a pathway that could direct RhoB towards a tumor-suppressive or -promoting function [66]. The association of TSA delivery nanosystems with that of tamoxifen or pure antiestrogen that we have developed [61, 78] may synergise the therapeutic activity of each nanovector mainly in the case of ERβ expression, as illustrated by in vitro experiments [41]. Moreover, TSA liposomes should offer an innovative alternative strategy for the treatment of tamoxifen-resistant breast cancers in which Erb-B2 is overexpressed, such as in SKBr-3 cells, as well as in patients not responding to standard therapies.

Acknowledgements

The authors thank J. Mester for critical discussions and reading of the manuscript, A-M. Faussat (IFR Saint-Antoine, Paris, France) for flow cytometry experiments, and the animal facility service of the IFR 141 (Châtenay-Malabry, France).

Conflicts of interest statement

Authors' conflict of interest disclosure: None declared.
Funding: Financial support was obtained from the Centre National de la Recherche Scientifique, the Université Paris-Sud and the Hauts-de-Seine committee from the Ligue Nationale Contre le Cancer (fellowship to GU, and grant to J-M R).

References

1. Koehler KF, Helguero LA, Haldosen LA, Warner M, Gustafsson JA. Reflections on the discovery and significance of estrogen receptor β. Endocr Rev 2005;26:465–78.
2. Helguero LA, Faulds MH, Gustafsson JA, Haldosen LA. Estrogen receptors alfa (ER_α) and beta (ER_β) differentially regulate proliferation and apoptosis of the normal murine mammary epithelial cell line HC11. Oncogene 2005;24:6605–16.
3. Pettersson K, Delaunay F, Gustafsson JA. Estrogen receptor β acts as a dominant regulator of estrogen signaling. Oncogene 2000;19:4970–8.
4. Strom A, Hartman J, Foster JS, Kietz S, Wimalasena J, Gustafsson JA. Estrogen receptor β inhibits 17β-estradiol-stimulated proliferation of the breast cancer cell line T47D. Proc Natl Acad Sci USA 2004;101:1566–71.
5. Lazennec G. Estrogen receptor β, a possible tumor suppressor involved in ovarian carcinogenesis. Cancer Lett 2006;231: 151–7.
6. Ali S, Coombes RC. Endocrine-responsive breast cancer and strategies for combating resistance. Nat Rev Cancer 2002;2: 101–12.
7. Keen JC, Davidson NE. The biology of breast carcinoma. Cancer 2003;97(3 Suppl):825–33.
8. Johnston SR. Clinical efforts to combine endocrine agents with targeted therapies against epidermal growth factor receptor/human epidermal growth factor receptor 2 and mammalian target of rapamycin in breast cancer. Clin Cancer Res 2006;12: 1061s–8s.
9. Archer SY, Hodin RA. Histone acetylation and cancer. Curr Opin Genet Dev 1999;9:171–4.
10. Van Lint C, Emiliani S, Verdin E. The expression of a small fraction of cellular genes is changed in response to histone hyperacetylation. Gene Expr 1996;5:245–53.
11. Sowa Y, Orita T, Minamikawa S, Nakano K, Mizuno T, Nomura H, Sakai T. Histone deacetylase inhibitor activates the WAF1/Cip1 gene promoter through the Sp1 sites. Biochem Biophys Res Commun 1997;241:142–50.
12. Marks P, Rifkind RA, Richon VM, Breslow R, Miller T, Kelly WK. Histone deacetylases and cancer: causes and therapies. Nat Rev Cancer 2001;1:194–202.
13. Palmieri C, Coombes RC, Vigushin DM. Targeted histone deacetylase inhibition for cancer prevention and therapy. Prog Drug Res 2005;63:147–81.

14. Minucci S, Pelicci PG. Histone deacetylase inhibitors and the promise of epigenetic (and more) treatments for cancer. Nat Rev Cancer 2006;6:38–51.
15. Bolden JE, Peart MJ, Johnstone RW. Anticancer activities of histone deacetylase inhibitors. Nat Rev Drug Discov 2006;5:769–84.
16. Grunstein M. Histone acetylation in chromatin structure and transcription. Nature 1997;389:349–52.
17. Roy S, Packman K, Jeffrey R, Tenniswood M. Histone deacetylase inhibitors differentially stabilize acetylated p53 and induce cell cycle arrest or apoptosis in prostate cancer cells. Cell Death Differ 2005;12:482–91.
18. Fu M, Rao M, Wang C, Sakamaki T, Wang J, Di Vizio D, Zhang X, Albanese C, Balk S, Chang C, Fan S, Rosen E, Palvimo JJ, Jänne OA, Muratoglu S, Avantaggiati ML, Pestell RG. Acetylation of androgen receptor enhances coactivator binding and promotes prostate cancer cell growth. Mol Cell Biol 2003;23: 8563–75.
19. Wang C, Fu M, Angeletti RH, Siconolfi-Baez L, Reutens AT, Albanese C, Lisanti MP, Katzenellenbogen BS, Kato S, Hopp T, Fuqua SA, Lopez GN, Kushner PJ, Pestell RG. Direct acetylation of the estrogen receptor α hinge region by p300 regulates transactivation and hormone sensitivity. J Biol Chem 2001;276: 18375–83.
20. Kim MY, Hsiao SJ, Kraus WL. A role for coactivators and histone acetylation in estrogen receptor α-mediated transcription initiation. EMBO J 2001;20:6084–94.
21. Reid G, Hubner MR, Metivier R, Brand H, Denger S, Manu D, Beaudouin J, Ellenberg J, Gannon F. Cyclic, proteasome-mediated turnover of unliganded and liganded ERα on responsive promoters is an integral feature of estrogen signaling. Mol Cell 2003;11:695–707.
22. Duong V, Licznar A, Margueron R, Boulle N, Busson M, Lacroix M, Katzenellenbogen BS, Cavailles V, Lazennec G. ERα and ERβ expression and transcriptional activity are differentially regulated by HDAC inhibitors. Oncogene 2006;25: 1799–806.
23. Duong V, Bret C, Altucci L, Mai A, Duraffourd C, Loubersac J, Harmand PO, Bonnet S, Valente S, Maudelonde T, Cavailles V, Boulle N. Specific activity of class II histone deacetylases in human breast cancer cells. Mol Cancer Res 2008;6:1908–19.
24. Kim TY, Bang YJ, Robertson KD. Histone deacetylase inhibitors for cancer therapy. Epigenetics 2006;1:14–23.
25. Keen JC, Yan L, Mack KM, Pettit C, Smith D, Sharma D, Davidson NE. A novel histone deacetylase inhibitor, scriptaid, enhances expression of functional estrogen receptor α (ER) in ER negative human breast cancer cells in combination with 5-aza 2'-deoxycytidine. Breast Cancer Res Treat 2003;81:177–86.
26. Bhat-Nakshatri P, Wang G, Appaiah H, Luktuke N, Carroll JS, Geistlinger TR, Brown M, Badve S, Liu Y, Nakshatri H. AKT alters genome-wide estrogen receptor α binding and impacts estrogen signaling in breast cancer. Mol Cell Biol 2008;28: 7487–503.
27. Hamner JB, Sims TL, Cutshaw A, Dickson PV, Rosati S, McGee M, Ng CY, Davidoff AM. The efficacy of combination therapy using adeno-associated virus–interferon β and trichostatin A in vitro and in a murine model of neuroblastoma. J Pediatr Surg 2008;43:177–82; discussion 182–3.
28. Vanhaecke T, Papeleu P, Elaut G, Rogiers V. Trichostatin A-like hydroxamate histone deacetylase inhibitors as therapeutic agents: toxicological point of view. Curr Med Chem 2004;11: 1629–43.
29. Elaut G, Torok G, Vinken M, Laus G, Papeleu P, Tourwe D, Rogiers V. Major phase I biotransformation pathways of trichostatin A in rat hepatocytes and in rat and human liver microsomes. Drug Metab Dispos 2002;30:1320–8.
30. Urbinati G, Marsaud V, Plassat V, Fattal E, Lesieur S, Renoir JM. Liposomes loaded with histone deacetylase inhibitors for breast cancer therapy. Int J Pharm 2010;397:184–93.
31. Maillard S, Ameller T, Gauduchon J, Gougelet A, Gouilleux F, Legrand P, Marsaud V, Fattal E, Sola B, Renoir JM. Innovative drug delivery nanosystems improve the anti-tumor activity in vitro and in vivo of anti-estrogens in human breast cancer and multiple myeloma. J Steroid Biochem Mol Biol 2005;94:111–21.
32. Marsaud V, Gougelet A, Maillard S, Renoir JM. Various phosphorylation pathways, depending on agonist and antagonist binding to endogenous estrogen receptor α (ERα), differentially affect ERα extractability, proteasome-mediated stability, and transcriptional activity in human breast cancer cells. Mol Endocrinol 2003;17:2013–27.
33. Plassat V, Martina MS, Barratt G, Menager C, Lesieur S. Sterically stabilized superparamagnetic liposomes for MR imaging and cancer therapy: pharmacokinetics and biodistribution. Int J Pharm 2007;344:118–27.
34. Bouclier C, Marsaud V, Bawa O, Nicolas V, Moine L, Opolon P, Renoir JM. Coadministration of nanosystems of short silencing RNAs targeting oestrogen receptor α and anti-oestrogen synergistically induces tumor growth inhibition in human breast cancer xenografts. Breast Cancer Res Treat 2009;122:145–58.
35. Abramova MV, Pospelova TV, Nikulenkov FP, Hollander CM, Fornace AJ Jr, Pospelov VA. G1/S arrest induced by histone deacetylase inhibitor sodium butyrate in E1A + Ras-transformed cells is mediated through down-regulation of E2F activity and stabilization of β-catenin. J Biol Chem 2006;281:21040–51.
36. Alao JP, Lam EW, Ali S, Buluwela L, Bordogna W, Lockey P, Varshochi R, Stavropoulou AV, Coombes RC, Vigushin DM. Histone deacetylase inhibitor trichostatin A represses estrogen receptor α-dependent transcription and promotes proteasomal degradation of cyclin D1 in human breast carcinoma cell lines. Clin Cancer Res 2004;10:8094–104.
37. Archer SY, Meng S, Shei A, Hodin RA. $p21^{WAF1}$ is required for butyrate-mediated growth inhibition of human colon cancer cells. Proc Natl Acad Sci USA 1998;95:6791–6.
38. Richon VM, Sandhoff TW, Rifkind RA, Marks PA. Histone deacetylase inhibitor selectively induces $p21^{WAF1}$ expression and gene-associated histone acetylation. Proc Natl Acad Sci USA 2000;97:10014–9.
39. Bali P, Pranpat M, Swaby R, Fiskus W, Yamaguchi H, Balasis M, Rocha K, Wang HG, Richon V, Bhalla K. Activity of suberoylanilide hydroxamic acid against human breast cancer cells with amplification of her-2. Clin Cancer Res 2005;11:6382–9.
40. Liu A, Cerniglia GJ, Bernhard EJ, Prendergast GC. RhoB is required to mediate apoptosis in neoplastically transformed cells after DNA damage. Proc Natl Acad Sci USA 2001;98:6192–7.
41. Hodges-Gallagher L, Valentine CD, Bader SE, Kushner PJ. Inhibition of histone deacetylase enhances the anti-proliferative action of antiestrogens on breast cancer cells and blocks tamoxifen-induced proliferation of uterine cells. Breast Cancer Res Treat 2007;105:297–309.
42. Sharma D, Saxena NK, Davidson NE, Vertino PM. Restoration of tamoxifen sensitivity in estrogen receptor-negative breast cancer cells: tamoxifen-bound reactivated ER recruits distinctive corepressor complexes. Cancer Res 2006;66:6370–8.
43. Jang ER, Lim SJ, Lee ES, Jeong G, Kim TY, Bang YJ, Lee JS. The histone deacetylase inhibitor trichostatin A sensitizes estrogen receptor α-negative breast cancer cells to tamoxifen. Oncogene 2004;23:1724–36.
44. Fiskus W, Ren Y, Mohapatra A, Bali P, Mandawat A, Rao R.

Herger B, Yang Y, Atadja P, Wu J, Bhalla K. Hydroxamic acid analogue histone deacetylase inhibitors attenuate estrogen receptor-α levels and transcriptional activity: a result of hyperacetylation and inhibition of chaperone function of heat shock protein 90. Clin Cancer Res 2007;13:4882–90.
45. Nakajima S, Niizeki H, Tada M, Nakagawa K, Kondo S, Okada F, Kobayashi M. Trichostatin A with adenovirus-mediated p53 gene transfer synergistically induces apoptosis in breast cancer cell line MDA-MB-231. Oncol Rep 2009;22:143–8.
46. Delarue FL, Adnane J, Joshi B, Blaskovich MA, Wang DA, Hawker J, Bizouarn F, Ohkanda J, Zhu K, Hamilton AD, Chellappan S, Sebti SM. Farnesyltransferase and geranylgeranyltransferase I inhibitors upregulate RhoB expression by HDAC1 dissociation, HAT association and histone acetylation of the RhoB promoter. Oncogene 2007;26:633–40.
47. Sharma D, Blum J, Yang X, Beaulieu N, Macleod AR, Davidson NE. Release of methyl CpG binding proteins and histone deacetylase 1 from the estrogen receptor α (ER) promoter upon reactivation in ER-negative human breast cancer cells. Mol Endocrinol 2005;19:1740–51.
48. Janicke RU, Sprengart ML, Wati MR, Porter AG. Caspase-3 is required for DNA fragmentation and morphological changes associated with apoptosis. J Biol Chem 1998;273:9357–60.
49. Liang Y, Yan C, Schor NF. Apoptosis in the absence of caspase 3. Oncogene 2001;20:6570–8.
50. Moghimi SM, Szebeni J. Stealth liposomes and long circulating nanoparticles: critical issues in pharmacokinetics, opsonization and protein-binding properties. Prog Lipid Res 2003;42:463–78.
51. Moghimi SM, Hunter AC, Murray JC. Long-circulating and target-specific nanoparticles: theory to practice. Pharmacol Rev 2001;53:283–318.
52. Qiu L, Kelso MJ, Hansen C, West ML, Fairlie DP, Parsons PG. Anti-tumour activity in vitro and in vivo of selective differentiating agents containing hydroxamate. Br J Cancer 1999;80:1252–8.
53. Hanahan D, Weinberg RA. The hallmarks of cancer. Cell 2000;100:57–70.
54. Liu TC, Castelo-Branco P, Rabkin SD, Martuza RL. Trichostatin A and oncolytic HSV combination therapy shows enhanced antitumoral and antiangiogenic effects. Mol Ther 2008;16:1041–7.
55. Vigushin DM, Ali S, Pace PE, Mirsaidi N, Ito K, Adcock I, Coombes RC. Trichostatin A is a histone deacetylase inhibitor with potent antitumor activity against breast cancer in vivo. Clin Cancer Res 2001;7:971–6.
56. Canes D, Chiang GJ, Billmeyer BR, Austin CA, Kosakowski M, Rieger-Christ KM, Libertino JA, Summerhayes IC. Histone deacetylase inhibitors upregulate plakoglobin expression in bladder carcinoma cells and display antineoplastic activity in vitro and in vivo. Int J Cancer 2005;113:841–8.
57. Dokmanovic M, Marks PA. Prospects: histone deacetylase inhibitors. J Cell Biochem 2005;96:293–304.
58. Prendergast GC. Actin' up: RhoB in cancer and apoptosis. Nat Rev Cancer 2001;1:162–8.
59. Fritz G, Kaina B. Ras-related GTPase RhoB represses NF-κB signaling. J Biol Chem 2001;276:3115–22.
60. Wang L, Yang L, Luo Y, Zheng Y. A novel strategy for specifically down-regulating individual Rho GTPase activity in tumor cells. J Biol Chem 2003;278:44617–25.
61. Renoir JM, Stella B, Ameller T, Connault E, Opolon P, Marsaud V. Improved anti-tumoral capacity of mixed and pure anti-oestrogens in breast cancer cell xenografts after their administration by entrapment in colloidal nanosystems. J Steroid Biochem Mol Biol 2006;102:114–27.
62. Yuan F, Leunig M, Huang SK, Berk DA, Papahadjopoulos D, Jain RK. Microvascular permeability and interstitial penetration of sterically stabilized (stealth) liposomes in a human tumor xenograft. Cancer Res 1994;54:3352–6.
63. Margueron R, Licznar A, Lazennec G, Vignon F, Cavailles V. Oestrogen receptor α increases $p21^{WAF1/CIP1}$ gene expression and the antiproliferative activity of histone deacetylase inhibitors in human breast cancer cells. J Endocrinol 2003;179:41–53.
64. Couderc B, Pradines A, Rafii A, Golzio M, Deviers A, Allal C, Berg D, Penary M, Teissie J, Favre G. In vivo restoration of RhoB expression leads to ovarian tumor regression. Cancer Gene Ther 2008;15:456–64.
65. Mazieres J, Tillement V, Allal C, Clanet C, Bobin L, Chen Z, Sebti SM, Favre G, Pradines A. Geranylgeranylated, but not farnesylated, RhoB suppresses Ras transformation of NIH-3T3 cells. Exp Cell Res 2005;304:354–64.
66. Doisneau-Sixou SF, Sergio CM, Carroll JS, Hui R, Musgrove EA, Sutherland RL. Estrogen and antiestrogen regulation of cell cycle progression in breast cancer cells. Endocr Relat Cancer 2003;10:179–86.
67. Jaffe AB, Hall A. Rho GTPases in transformation and metastasis. Adv Cancer Res 2002;84:57–80.
68. Karlsson R, Pedersen ED, Wang Z, Brakebusch C. Rho GTPase function in tumorigenesis. Biochim Biophys Acta 2009;1796:91–8.
69. Jahner D, Hunter T. The *ras*-related gene *rhoB* is an immediate-early gene inducible by v-Fps, epidermal growth factor, and platelet-derived growth factor in rat fibroblasts. Mol Cell Biol 1991;11:3682–90.
70. Heasman SJ, Ridley AJ. Mammalian Rho GTPases: new insights into their functions from in vivo studies. Nat Rev Mol Cell Biol 2008;9:690–701.
71. Adnane J, Muro-Cacho C, Mathews L, Sebti SM, Munoz-Antonia T. Suppression of rho B expression in invasive carcinoma from head and neck cancer patients. Clin Cancer Res 2002;8:2225–32.
72. Buck MB, Pfizenmaier K, Knabbe C. Antiestrogens induce growth inhibition by sequential activation of p38 mitogen-activated protein kinase and transforming growth factor-β pathways in human breast cancer cells. Mol Endocrinol 2004;18:1643–57.
73. Li H, Liu JP. Mechanisms of action of TGF-β in cancer: evidence for Smad3 as a repressor of the hTERT gene. Ann NY Acad Sci 2007;1114:56–68.
74. Muraoka-Cook RS, Dumont N, Arteaga CL. Dual role of transforming growth factor β in mammary tumorigenesis and metastatic progression. Clin Cancer Res 2005;11:937s–43s.
75. Bellizzi A, Mangia A, Chiriatti A, Petroni S, Quaranta M, Schittulli F, Malfettone A, Cardone RA, Paradiso A, Reshkin SJ. RhoA protein expression in primary breast cancers and matched lymphocytes is associated with progression of the disease. Int J Mol Med 2008;22:25–31.
76. Fritz G, Brachetti C, Bahlmann F, Schmidt M, Kaina B. Rho GTPases in human breast tumours: expression and mutation analyses and correlation with clinical parameters. Br J Cancer 2002;87:635–44.
77. Fan J, Yin WJ, Lu JS, Wang L, Wu J, Wu FY, Di GH, Shen ZZ, Shao ZM. ER α negative breast cancer cells restore response to endocrine therapy by combination treatment with both HDAC inhibitor and DNMT inhibitor. J Cancer Res Clin Oncol 2008;134:883–90.
78. Urbinati G, Audisio D, Marsaud V, Plassat V, Arpicco S, Sola B, Fattal E, Renoir JM. Therapeutic potential of new 4-hydroxytamoxifen-loaded pH-gradient liposomes in a multiple myeloma experimental model. Pharm Res 2009;27:327–39.